REPRODUCIBLE COMPUTATION

Received: 3 June 2023 | Accepted: 28 November 2024 | Online: 23 December 2024

JOURNAL OF GEOPHYSICS
Est. 1924
www.geophysicsjournal.com

A star's shut–vent magnetism buffer against incoming stars cuts stellar multiplicity, kills dwarf binaries

Sun dims as failed star Jupiter tries to go full-on pulsar

M. Omerbashich[1*]

[1)] Geophysics Online, 3501 Jack Northrop Ave, Ste. 6172, Los Angeles CA 90250

Cite as:
Omerbashich M. (2024) Sun dims as failed star Jupiter tries to go full-on pulsar. *J. Geophys.* 66:15–24.

Data for this article are in repo at: dx.doi.org/10.21227/cv28-8929

LSSA v.5 can be obtained at the U of New Brunswick: unb.ca/gge/Research/GRL/LSSA/sourceCode.html

PRESS RELEASE Read the PR for this article

A Sun–Jupiter decade-scale magnetic tangling appears from Wilcox Solar Observatory 1975–2021, N–S≲150 μT mean field data as a global response of solar magnetic fields to the recently discovered pulsar-like varying evolution of Jupiter global magnetoactivity in the 385.8–64.3 nHz (1–180-day) band of Rieger resonance of the solar wind since 2001. The Jovian sudden deviation has been so high at an extreme ≲20% field variance that it appears to have forced solar magnetoactivity devolution into an inverse-matching response at an effectively moderate ≲1.5% mean field variance. Thus, as Jupiter's decadal magnetoactivity evolved in a rare, increasingly sinusoidal fashion, seen in astronomy not only in magnetars but dwarf-novae as well, the Sun began reducing its magnetoactivity in a decreasingly sinusoidal fashion ~2002 (the epoch of Abbe number drop) to the solar cycle 24 extreme minimum. For a check, 2004–2021 WIND spacecraft data revealed a <0.5-var% (<5-dB) calm ≲50 nT interplanetary magnetic field at L1, slightly undulated by the Jupiter evolution. This revelation excluded the solar wind or the Sun as impulse sources, which agrees with the statistical fidelity waning down Jupiter–L1–Sun diffusion vector spaces, as 10^7–10^3–10^2. Magnetic tangling of stars with their hot (<0.1 AU) Jupiters was blamed in the past for observed star pulsation and superflaring 10^2–10^7 times more energetic than the strongest solar flare. Accordingly, the Sun's apparent ante-impulse locking creates a shock-absorbing mechanism—a routine Sun shutter response to Jupiter's remnant yet recurrent attempted phasing into the flare-brown-dwarf state—with which the Sun enters a grand minimum (sleep mode). I then propose that, since the mechanism must be primordial, Jupiter intermittently becomes an indirect driver of climate on Earth as the Sun prepares to discharge the mechanism-stored energy as a non-extinction ~10^{32}-erg superflare (currently overdue). At the same time, this shutting-venting magnetism buffer represents a universal stellar defense mechanism by which stars repel other (active and inactive) incoming stars. The discovery explains Milky Way observations of the ~1:3 relative scarcity of companion-stars systems and why binaries, and progressively multinaries, occur more often with the stellar mass increase, i.e., as this sifting mechanism—remarkably efficient in dwarfs as predominant yet less massive star type—naturally weakens, yielding to gravity. The mechanism could be vital to our understanding of the origin of Jupiter, star formation processes, and the nature of gravity.

Key words—Sun activity; solar grand minima; solar superflares; Sun–Jupiter tangling; Sun; Jupiter; stellar multiplicity; binary star systems.

HIGHLIGHTS

- Continuation study of the finding that Jupiter is a failed star and a *pulsing planet* from *in situ* data at Jupiter & Saturn (in this issue)
- Jupiter's jump from gaseous planet to primordial star state is compensated by the Sun dimming its magnetic activity to a grand minimum
- As Jupiter's magnetism changes decreasingly sinusoidally over decades like prebursting magnetars, the Sun's does increasingly sinusoidally
- Since the prebursting sequence involved in it is a universal primordial dynamic, this "camera shutter" mechanism is universal too
- The suppressed stored energy eventually gets released as a solar superflare, which occurs around twice a millennium (currently overdue)
- The *shut→vent* mechanism, like a magnetism buffer, shields stars against incoming active and inactive less massive stars, destroys binaries
- Global tangling between the star host and a guest is why binary stellar systems are much rarer amongst low-mass stars (most stars)
- As a primordial universal phenomenon (unlikely to ever go away), the mechanism stresses the need to monitor Jupiter permanently.

1. INTRODUCTION

While magnetic field interaction between stars and planets is likely complex, it has been established previously on large samples of Sun-like stars and their hot (roughly: those orbiting the primary star at <0.1 AU; with orbital periods <10 Earth days) Jupiters that geodynamical properties of a planet tend to be deducible from its detailed magnetic properties (Scharf, 2010). However, while that relationship does hold for some stars, the trend could be traced back to selection effects related to the planet detection efficiency (Poppenhaeger et al., 2010; Poppenhaeger & Schmitt, 2011). Namely, the search for exoplanets is necessarily biased as we find only the massive close-in planets around active stars, while even in nearby active stars the small remote planets go undetected (Poppenhaeger, 2015). We cannot at present then rule out if undetectable warm (roughly at 0.1–1

[*)] Correspondence to: omerbashich@geophysicsonline.org, hm@royalfamily.ba.

AU) or even cold (roughly at 1–10 AU) Jupiters could also cause such effects. Indeed, it is remarkable that a hot Jupiter can affect the host star dynamically by causing the star to pulsate harmonically at multiples of the planet's orbital frequency (de Wit et al., 2017). Again, no such effect of warm/cold Jupiters on stars is presently known, not because it does not exist but because such Jupiters are very difficult to detect. This unfortunate situation calls for studies of magnetic interaction between our Sun and Jupiter, especially because decade-scale *in situ* measurements for the first time are now available for both bodies.

If Jupiter does affect the Sun magnetically, it also affects other planets in between, including Mars and Earth with its Moon. Then, after suspecting that increased Jupiter magnetoactivity facilitates Martian seismicity (Omerbashich, 2023b), Omerbashich (2024) has demonstrated magnetar/novae-type ~2001–onward evolution of Jupiter's global magnetoactivity and compared this evolution to that of Saturn as the most similar gaseous giant in our solar system. The Saturn magnetic field has turned out to be tranquil over the same interval, which left an increased Jupiter magnetoactivity as the source of not only seismicity and other geodynamic phenomena (Omerbashich, 2023a; 2023b) but possibly of erupting solar superflares and pulsar-beam energy jets potentially dangerous to Earth as well.

Namely, while energetic events such as the star superflaring have been observed, as emitting up to 10^{38} erg or 10^{2}–10^{7} times more energy than most energetic solar flares (Rubenstein & Schaefer, 2000), the geological record over the past 2k yr contains no evidence of superflaring of our Sun (Schaefer et al., 2000). However, 10^{33}-erg (non-extinction) events are known to occur as often as every ~500-600 yr (Maehara et al., 2015), and our Sun does appear to set off 10^{32}-erg such events once every ~450 yr (Tsurutani et al., 2003). Since, over the past ~500 yr, the Earth lacked global aurorae as natural companion events of such superflares (Rubenstein & Schaefer, 2000), this type of superflaring on the Sun seems overdue. In addition, superflaring can emerge in a flare star (including subgiant dwarfs) due to magnetic energy stored in the atmosphere and possibly mass transfers (Pettersen, 1989). Kepler mission data confirmed that star flaring is a side effect of magnetism by showing that superflares arise on stars with large starspots, but had also observed no hot Jupiters around those stars, thus questioning the current models that predict that ~10% of such stars should have hot Jupiters (Maehara et al., 2012). Subsequent TESS mission data from a larger sample of stars (Tu et al., 2020) essentially confirmed the Kepler results. Besides, the current models were suspected to be incorrect because tidal locking would significantly weaken the magnetic fields of hot Jupiters (Griesmeier et al., 2004). Note that if Jupiter affects the Sun geodynamically (in the frequency space; in a pulsar-like fashion), modeling their magnetic tangling using magnetohydrodynamics (MHD) theory (Alfvén, 1942) as currently the only available tool would perhaps be unattainable for *pulsar Jupiter* (Omerbashich, 2024) since MHD is an approximate theory inapplicable to magnetospheres of pulsars (Spruit, 2017). Therefore, the magnetic tangling employed in the present study is not necessarily the same as that classically understood or speculated on within the framework of MHD. Classically and here, data collected *in situ* are considered a defining constraint of any theory without exception.

Thus, in what follows, I inspect if the detected Jovian pulsar-type bursting evolution (Omerbashich, 2024) means just the phasing into a flare star (sub-brown dwarf) state or the onset of a solar superflare or both. I then compare the pulsar character of Jupiter to the Sun and examine if the two have magnetically tangled on decadal scales (and thereby entangled). Omerbashich (2024) mapped the Jupiter magnetic field's global dynamics temporally by the mean-annual effects of that field on the surrounding solar wind (therein used as a proxy) and vice versa. For that purpose, computed were mean spectra of annual magnetospheric samplings in the 1–6-month (385.8–64.3 nHz) band of wind's Rieger mechanical resonance (RR)—a regular yet nonlinear flapping of solar particle ejecta blanketing the ecliptic (Omerbashich, 2024). Therefore, I also examine solar magnetoactivity for comparison in the present study in the band of RR.

2. Data & Methodology

To study the evolution of overall solar magnetoactivity, I use the Sun's (both hemispheres) diurnal ≲150 μT Mean Magnetic Field (MMF) data from the Wilcox Solar Observatory (WSO) (Scherrer et al., 1977; ref. Acknowledgments). The background field dominates the MMF in a ~9:1 ratio to other magnetic features, including local fields, i.e., sunspots (Bose & Nagaraju, 2018). Since primarily weather conditions controlled the ability to collect data, parts of the record during the summer months were complete, with the remaining portion nearly complete (>90%). Because the telescope operated with a reduced polarization sensitivity due to lens contamination during the 16 December 2016–18 May 2017 interval when therefore the record did not reflect recalibrated MMF values so that only approximate errors are available, possibly making the field samplings nonlinearly noisy, I discard the data from that interval. The analyzed data spanned the WSO record from the start, on 16 May 1975, through 3 August 2021 inclusively.

To temporally map the hyperlow-frequency (<1μHz) dynamics of the solar wind, I spectrally analyze ≲50 nT (≲20 nT most of the time) total-field magnetometer recordings collected between 1995–2021 by the WIND mission (Lepping et al., 1995; ref. Acknowledgments). As in the Jupiter study by Omerbashich (2024), the 1–6-month was again the spectral band of choice since it reflects the most energetic dynamics (interplanetary dynamics as normalized to the Earth case). After spending most of the initial operational time in a lunar orbit, the spacecraft has been sampling unperturbed interplanetary magnetic field (IMF) in a short fixed orbit at the Lagrangian point L1 since May 2004.

Spectral magnitudes in the present study were computed in both percentages of respective peak's contribution to data variance (var%) and decibels (dB), using the rigorous Gauss–Vaníček (G–V) method of spectral analysis (GVSA) by Vaníček (1969, 1971), and plotted against linear background noise levels. GVSA comes integrated with a complete statistical analysis toolbox into a scientific software package LSSA that provides periodicity estimates in the strictly least-squares sense, unlike the more popular Lomb–Scargle approximation that underperforms when analyzing noisy and complicated signals, such as those of solar activity (Carbonell et al., 1992; Danilović

et al., 2005). Tests of GVSA, showing its superiority, have been performed, e.g., by Taylor & Hamilton (1972) and Omerbashich (2003). GVSA has many benefits, including advantages over Fourier methods (Omerbashich, 2021, 2007, 2006; Press et al., 2007; Pagiatakis, 1999; Wells et al., 1985). By discarding non-recalibrated data in the record, I also take advantage of the blindness to data gaps as a feature exclusive to the least-squares class of spectral analysis techniques.

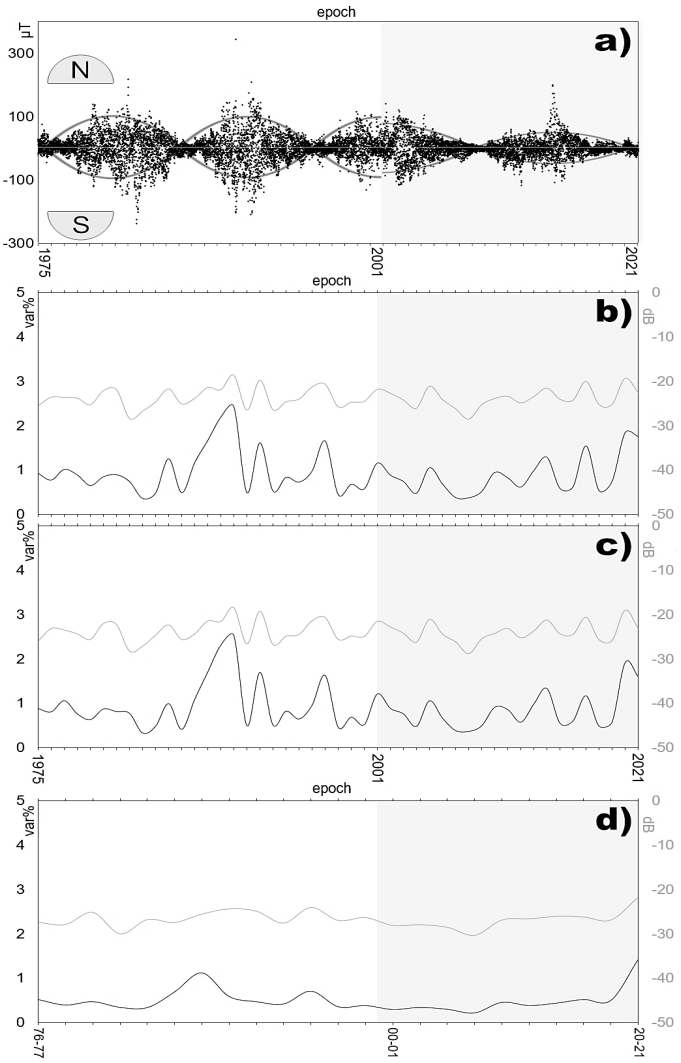

Figure 1. Sun's overall magnetoactivity since 1975. Panel a: diurnal variations of the mean magnetic field (MMF) from the Wilcox Solar Observatory, in μT, depicting sudden (controlled) Sun-wide dampening of field oscillations from ~2002 on, which coincided in time with the onset of ~2001–onward magnetar-type evolution of Jupiter global magnetoactivity (Omerbashich, 2024). The sudden systematic drop in the Sun's global magnetoactivity is already noticeable here in the time domain, as pre-2002 (on white background) vs. post-2001 (on gray background) evolution envelope. Panel b: Sun overall magnetoactivity evolution as a change of mean-annual Gauss–Vaníček (G–V) spectral magnitude in var% (solid line) and dB (gray) of field variations from panel (a), 30–180-day (385.8–64.3 nHz) band. The depicted solar overall magnetoactivity appears to show the Sun's response to a globally forced (extrasolar) event since ~2002, in the form of an ante-signal to the Jovian such evolution as extracted by Omerbashich (2024), indicating that the Sun compensated for the sudden energy surplus by lowering its activity, to a record minimum already in solar cycle 24. Panels (c)–(d): an examination of signal strength and clarity, by moving the band's lower end: (a) shortening to 30–140-day to exclude the Rieger period and leave Rieger harmonics only, and (d) expanding to 30–300-day (and data then to 2-yr bins) to include the first mid-term Rieger reflection (Bai, 2003). The shortening affected signal clarity so the supposed ante-impulse could be recovered when considering the whole Rieger resonance (RR) only. The expansion has affected the signal by virtually extinguishing it, confirming that only the RR band enables recovery of the ante-impulse. Thus, the Rieger band serves as a natural band of the overall solar activity, with the Rieger period as the fundamental note, as perceived externally to the Sun. Gray boxes: the time interval of the Jupiter evolution impulse and the presupposed Sun ante-impulse. For the data source for panel (a), see Acknowledgments. Data for panels (b)–(c) are in Table 1.

The same as in the demonstration of increased Jupiter magnetoactivity by Omerbashich (2024), the change in mean magnetic field activity of the Sun (generation of electromagnetic radiation and sunspots—"dark" or relatively dimmer and less magnetically active surface regions) is in the present study discerned by using a spectral method for measuring field dynamics (Omerbashich, 2003, 2007, 2009). In that method, unlike in classically performed comparisons of ratios of Fourier spectral amplitudes to discern field dynamics, average G–V variance-spectra over some band of interest, since already directly energy-stratified, represent field dynamics over an epoch of sampling. As for Jupiter, the 30–180-day (common) spectral band of solar-wind resonance is used in the present study to represent field magnetoactivity, while one Earth year is again the epoch of choice. Refer to Omerbashich (2024; 2023a) for details on GVSA implementation in studying the global dynamics of magnetic activity of Jupiter and the Sun, respectively.

3. Results

The solar mean magnetic field responded around 2002 to the Jovian signal in the seemingly same but inverted manner, Fig. 1. If this response was genuine, the Sun magnetism has virtually compensated for the signal by entering into a decreasingly sinusoidal mode, revealing that the two magnetic fields had effectively entangled a very long time ago, so they tangle complexly since. The ante-impulse signature may reflect an influx of energy absorbed by a general and well-tuned oscillatory system. Akin to a car shock absorber, the entanglement would represent compensatory dynamics occurring on spatially global and temporally decadal scales. It is then only natural to deduce that this compensation also could encompass the observed lowering of solar activity that soon after ensued in solar cycle 24. However, due to (also natural) insufficient dampening under inherently resonant and chaotic overall dynamics of the Sun (Omerbashich, 2024), incoming energy is never fully absorbed and has to be released somehow to maintain system stability. This state is then possibly observed as the ante-impulse decreasingly sinusoidal evolution, e.g., in pulsar 4U 0142+61 (Gonzalez et al., 2010), as it was preparing to release surplus stored magnetic energy or a superburst. The same then could be expected of the Sun, so its response mechanism to Jupiter's pulsation phase may at the same time be the Sun's superflaring mechanism. Note that there exist other, albeit in nature rarely, cases of decreasingly sinusoidal (increasingly pulsating) mode of energy diffusion. One example is the preparation stage of explosive discharge imminent in compressively overloaded closed physical systems.

As seen in more detail in Fig. 2, the Sun has thus virtually compensated for the Jupiter impulse with the subsequent solar cycle 24 that began in 2009, including the lowering of solar activity. So the Sun–Jupiter decade-scale magnetic entanglement could provide a physical explanation for the observed record-low solar activity of the last decade, starting with the 2014 maximum of the cycle 24 and the preceding minimum of 2009 (Fig. 2-a), both being among the weakest on proxy record (Basu, 2013) and weakest on instrumented record. In a study of

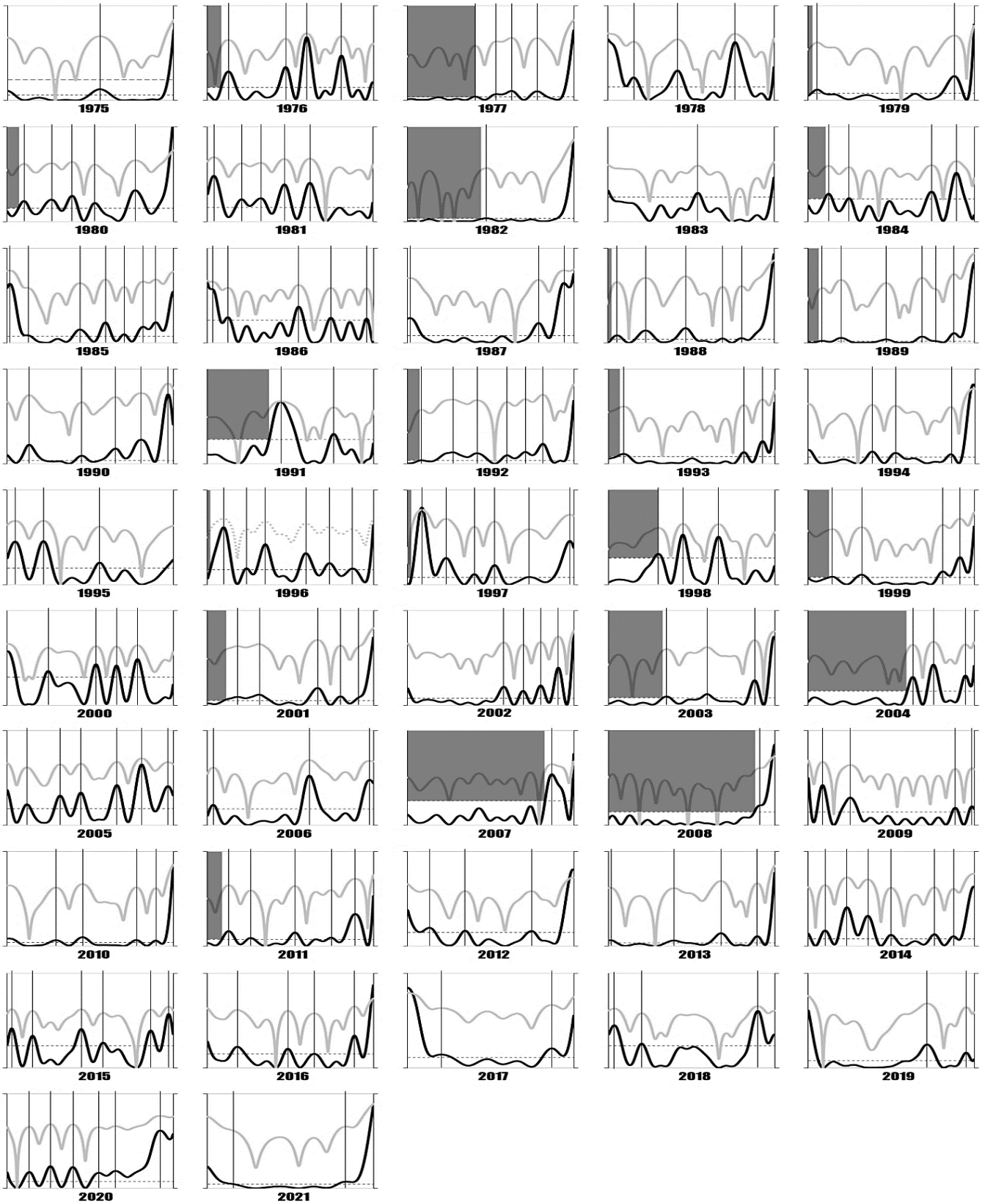

Figure 2. A blind-plot stack of MMF's G–V spectra in var% (dark lines) and dB (light lines), showing mixed-rate (highly turbulent) anisotropic peak splitting under Sun magnetoactivity since 1975. The overwhelming increase in Jupiter magnetoactivity past ~2002 coincides with the epochs of extinguished lowest frequencies that reflect the most energetic mean-field dynamics (gray boxes). Primarily due to the absence of global turbulent fields, the Jupiter case features no such systematic (prolonged) extinguishing in the lowest frequencies; see Fig. 3–right panel by Omerbashich (2024). The return of low-frequency spectral contents in 2009 and on coincided with the Sun (by then) supposedly compensating the Jupiter impulse with the solar cycle 24 of 2009, i.e., lowering of solar activity. Note that at least one case, that of 1977, i.e., the absence of low-frequency spectral contents therein, was due to the solar cycle 21 minimum. Amplitudes are not to scale. The short-dashed line marks significance at the 67% level, which practically coincides with the abscissa in most panels, with the 99% level always nearby (shown long-dashed on the 1975 plot for illustration). See Supplement for data.

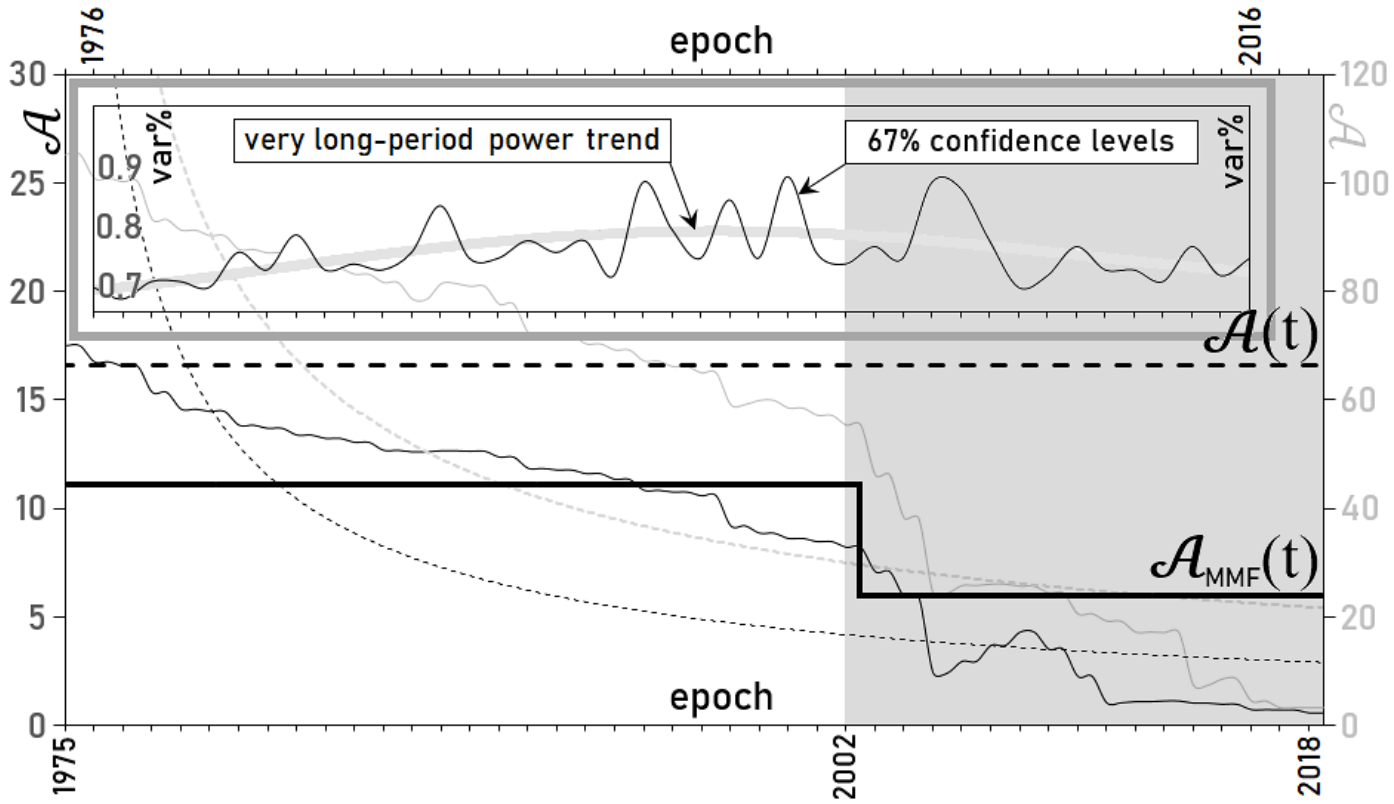

Figure 3. Plots of scaled Abbe numbers, $\mathcal{A}$, for the time series from Table 1, of G–V epoch-mean spectra of 1975–2021 Wilcox Solar Observatory MMF diurnal data. The drop epoch was determined by shifting (shortening) the time series one epoch at a time, and on through 2019: for mean variance-spectra—thin dark line with power trend as dark-dotted, and for mean power-spectra—thin light line with power trend as light-dotted. Note that the downward linear trend (not plotted) in the $\mathcal{A}$ number from the shifted time series is due to data shortening and not genuine (see callout for an actual trend). Based on the drop epoch, thus determined as ~2002, $\mathcal{A}_{MMF}$(t) numbers were computed for pre-drop (1975–2002 conclusive) and post-drop (2003–2021) portions of the time series, Eq. (1)—thick step-line with the $\mathcal{A}$(t) of the total time-series (thick dashed). Comparing the two thick lines and in-between the steps confirms that the drop was sudden, so the post-drop portion of the time series describes the smoothest function (here varyingly sinusoidal). Note that the final plunge in $\mathcal{A}$ occurred in 2009, i.e., at the onset of solar cycle 24, further contributing to regular activity decrease. Gray box: time interval of the Sun's ante-impulse to Jupiter's evolution impulse, Fig. 1-b. *Callout*: plot of epochal 67%-significance levels from 1976–2016 (end-epochs with ≥1/2-yr data gaps omitted) in var%, showing the real (very long period-) power trend in the Sun internal energy dynamics as the thick gray curve, thanks to the G–V linear background noise levels even from raw data, and thus variance-spectra measuring system energy levels relatively (Omerbashich, 2003, 2007, 2009). The trend probably extends to centennial scales and reflects known global solar variations down to millennial scales, such as the Hallstatt cycle, of ~2400 yr, at which solar grand minima and maxima cluster (Usoskin et al., 2016).

the long-term evolution of solar activity, a proxy dataset spanning the last 11.5 kyr has shown that a stochastic (therefore not necessarily internal) process possibly drives the recurrence of solar grand minima/maxima; the same study showed that these events cluster in time, with long event-free periods between the clusters—indicating that the Sun dynamo is controlled by processes related to the accumulation and release of energy (Usoskin et al., 2007). The above two previous results combined support the here-proposed scenario under which Jupiter indeed phases in and out of its active states, each time pending sufficient accumulation of magnetic–rotational energy to the point of criticality. Then subsequent Jupiter–Sun magnetic reconnecting (possibly tidally-orbitally aided), occurring in a situation of increased Jovian magnetoactivity, makes the Sun compensate for reactivated pulsar Jupiter by lowering solar activity to the point of a grand minimum.

To statistically verify that the solar activity drop as seen in Fig. 1-b indeed was both sinusoidal and sudden, and to discern its timing, I compute the Abbe number, $\mathcal{A}$, which quantifies signal smoothness (or roughness) by comparing mean square successive differences of a time series x_i of $n \in \aleph$ values and the mean $\bar{x}$, against variance (von Neumann, 1941, 1942):

$$\mathcal{A} = \frac{n}{2(n-1)} \frac{\sum_{i=1}^{n-1}(x_{i+1} - x_i)^2}{\sum_{i=1}^{n}(x_i - \bar{x})^2}. \quad (1)$$

Generally, the Abbe number decreases as signal smoothness increases. As applied to the problem of the present study, Fig. 3, this verification turned out positive for both of the above-implied spatiotemporal manners in which the Sun magneto-activity devolved from 1975 to 2021.

To physically verify the directionality of Jupiter–L1–Sun impulse propagation down the respective vector spaces, I computed the IMF magnetoactivity at the Lagrangian point L1, midway between the Sun and the Earth. As it turned out, the IMF at L1 also appears to have responded to the signal past 2004, albeit only slightly so, Fig. 4. This negligible effect of the presupposed Jupiter–Sun tangling on the IMF—even though it would be orders of magnitude weaker than the overall Sun magnetism—would be expected since magnetic tangling generally can arise easier among homogenous mass bodies than the heterogeneous solar wind jets. To statistically verify the result for each estimated spectral peak, I use its fidelity values and compare the statistics from those three locations (Jupiter, Sun, L1), Fig. 5.

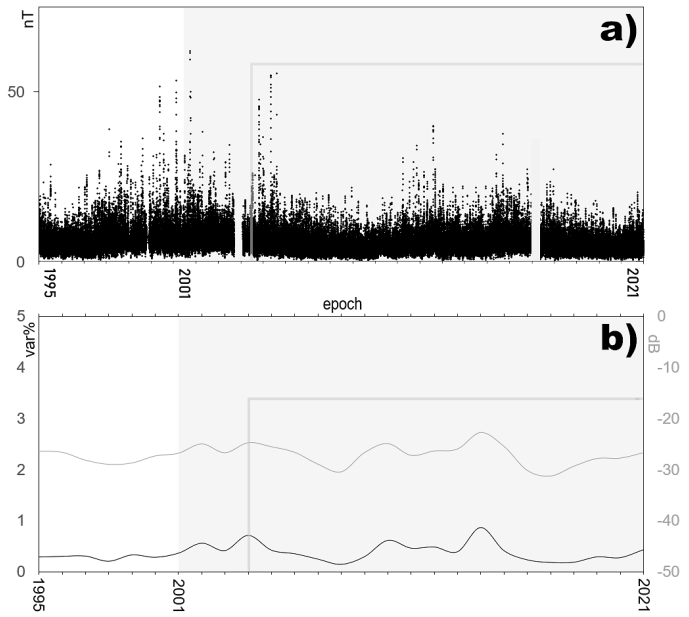

Figure 4. Panel a: 1995–2021 unperturbed ≲50 nT (<20 nT most of the time) interplanetary magnetic field (IMF) data from the WIND mission at the Lagrangian point L1 (in an L1-fixed quasi-orbit continuously since 2004). Panel b: G–V spectra (as for Fig. 1-b–d) revealed a <0.5-var% (<5-dB) calm IMF, as effectively slightly undulated by the Jupiter evolution impulse (here observed visually, since data size was insufficient for computations of relative Abbe number like those in Fig. 3). This result excludes both IMF and Sun as impulse sources: the former because L1 is closer to the Sun than Jupiter is yet considerably less affected by the impulse, and the latter because it is the source of the solar wind that ought then to preserve (or, shape the IMF at L1 into) the signature of such Sun-originating impulses if any. Gray box: time interval of the Jupiter evolution impulse and Sun ante-impulse. Gray frame: time interval of continuous coverage of IMF at L1 by WIND.

Year	var%	dB	Year	var%	dB	Year	var%	dB
1975	0.9	-25.5	1991	0.5	-26.5	2007	0.4	-26.2
1976	0.8	-23.6	1992	1.6	-19.7	2008	0.4	-28.6
1977	1.0	-23.7	1993	0.5	-26.5	2009	0.5	-25.3
1978	0.9	-23.8	1994	0.8	-24.7	2010	0.9	-23.9
1979	0.6	-25.3	1995	0.7	-24.0	2011	0.8	-23.4
1980	0.8	-22.1	1996	1.0	-21.3	2012	0.6	-24.9
1981	0.9	-21.9	1997	1.7	-20.7	2013	1.0	-23.5
1982	0.7	-28.4	1998	0.4	-25.8	2014	1.3	-21.5
1983	0.4	-26.8	1999	0.7	-24.8	2015	0.6	-24.1
1984	0.5	-24.7	2000	0.6	-24.6	2016	0.6	-24.3
1985	1.3	-21.7	2001	1.2	-21.8	2017	1.5	-20.0
1986	0.5	-25.1	2002	0.9	-22.7	2018	0.5	-25.3
1987	1.2	-23.9	2003	0.7	-24.2	2019	0.7	-25.2
1988	1.7	-21.4	2004	0.5	-26.1	2020	1.8	-19.3
1989	2.2	-21.9	2005	1.0	-21.1	2021	1.8	-22.5
1990	2.4	-18.6	2006	0.7	-24.2			

Table 1. Spectral values, Wilcox Solar Observatory solar mean magnetic field, Fig.1–a.

Year	var%	dB	Year	var%	dB	Year	var%	dB
1975	0.3	-26.4	1984	0.7	-24.7	1993	0.4	-25.9
1976	0.3	-26.6	1985	0.4	-25.5	1994	0.9	-22.7
1977	0.3	-28.1	1986	0.4	-26.6	1995	0.4	-25.4
1978	0.2	-28.9	1987	0.2	-28.9	1996	0.2	-30.1
1979	0.3	-28.6	1988	0.1	-30.4	1997	0.2	-31.2
1980	0.3	-27.3	1989	0.3	-26.6	1998	0.2	-29.3
1981	0.4	-26.8	1990	0.6	-24.9	1999	0.3	-27.8
1982	0.6	-24.9	1991	0.5	-27.2	2000	0.3	-27.7
1983	0.4	-26.7	1992	0.5	-26.3	2001	0.4	-26.6

Table 2. Spectral values, WIND mission interplanetary magnetic field (IMF) data, Fig. 4.

As seen in Fig. 5, fidelity on spectral-peak estimates stayed well within a very high ($\Phi \gg 12$) range, or 10^7–10^5 going from lowest- to highest-frequency spectral peaks, respectively (Omerbashich, 2024), where $\Phi > 12$ is indicative of a physical process (Omerbashich, 2006). Thus, the imprint of the Jovian global decade-scale magnetic field's activity onto the solar-wind dynamics in the band of Rieger-resonance appears to have been both total and incessant for all practical purposes. Note that the fidelity of the Saturn spectra (not shown) was over half an order magnitude below that of the Jupiter spectra, in the $3.7 \cdot 10^6$–10^5 range (Omerbashich, 2024), but still higher than for either the Sun or IMF at L1 (both nearly the same distance from Jupiter). Such discrepancy reflects an influence of the Jovian magnetic field on Saturn's magnetoactivity, as well as a vigor of RR near Saturn.

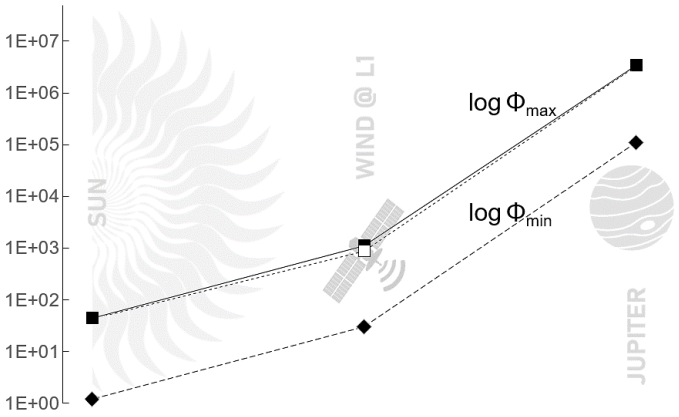

Figure 5. The plot of spatially changing maximum values (Φ_{max}—square markers) and minimum values (Φ_{min}—rhombus markers) of statistical fidelity, Φ, for frequency spectra of 2000–2021 RR. Left column—at the Sun (Wilcox Solar Observatory telescope MMF data); Middle—at the Lagrangian point L1 in IMF midway between the Earth and the Sun (WIND mission data since 2004 – white marker and dotted lines); Right—at Jupiter (Galileo, Cassini, Juno missions' data) from Omerbashich (2024). The drop appears to reflect the natural dissipation of Jupiter's magnetic energy so that the logarithmic representation maintains the range. While IMF strength varies greatly and is independent of the distance from the Sun, the depicted exponential (naturally upstream the solar wind) waning of fidelity down the impulse diffusion vector spaces Jupiter–L1–Sun, as 10^7–10^3–10^2 respectively, highlights Jupiter as the source of the emission and thus eliminates both the solar wind and the Sun as impulse sources.

In the Sun case (WSO data), fidelity was between 44–14 on the lowest and 5–1 on the highest frequencies. These values indicate that, within the band of interest, the Sun emitted energy only in the lowest (strongest-energy) frequencies, i.e., just about responded to an external process as the Sun was almost out of reach of the Jupiter impulse while the higher frequencies were sporadic and therefore uncharacteristic, Fig. 2. If real, the imprint of the Jupiter impulse onto the solar magnetosphere was thus incomplete but incessant.

In the IMF case (WIND data), fidelity was between 1100–360 on the lowest and 53–30 on the shortest frequencies, indicating that IMF at L1 was well within reach of the Jupiter very-long-period (decade-scale-) magnetic impulse to respond to it magnetically as well, i.e., to allow it to slightly moderate IMF amplitudes, Fig. 4.

Thus, statistical fidelity of the computed frequency spectra is seen as naturally (upstream the solar wind) diminishing down the impulse propagation vector spaces Jupiter–L1–Sun, as 10^7–10^3–10^2, respectively, Fig. 5. This directionality and gradual exponential drop indicate a genuine impulse and corroborate the impulse's general direction, thus supporting the physical interpretation of the result as the Sun's ante-impulse to Jupiter's decadal magnetoactivity increase ("the impulse").

Since Jupiter's magnetic field is rotational, the Jovian magnetosphere and associated pulsar energy emissions are moderated largely by incoming mass transfers, primarily from the solar wind. Besides, variance spectra as such are energy stratified. This situation justified taking the IMF variance, as represented by the RR variance spectra and its energy band, proportionate to the Jovian magnetic field variance. This logical extension forms the nature of the magnetic field's signature as impressed into the solar wind—used then as a proxy of global magnetoactivity. On the other hand, since the character of the Sun's overall magnetic activity remains extremely complex to decipher and thus hard to model or predict, the uncertainty in relating mean-field variance to a narrowed-field-variance as described spectrally in the band of interest is non-obvious, but here also of no concern given the relatively lower effective spectral response of the Sun. As in the Jupiter study, while the 99%-significance level in all cases was close to the 67%-significance level, the latter was considered sufficient for validating widely reported physical period ensembles like RR. Subsequently, such reasoning became justified additionally by those levels revealing a centennial trend, Fig. 3–callout.

4. Discussion

Rieger resonance (RR) of the solar wind arises due to the Sun's internal processes and gets modulated by the physics of planetary constellations acting as natural obstacles (Omerbashich, 2024). RR consists of the P_{Rg}=~154-day driver (Rieger et al., 1984) called the Rieger period, and its 5/6 P_{Rg}, 2/3 P_{Rg}, 1/2 P_{Rg}, 1/3 P_{Rg}, 1/4 P_{Rg}. 1/5 P_{Rg} harmonics or ~128, ~102, ~78, ~51, ~38, ~30-day periods called the Rieger-type periodicities (Dimitropoulou et al., 2008). A periodically forced damped nonlinear oscillator that exhibits periodic and chaotic behavior can model this resonance (Bai & Cliver, 1990). P_{Rg} and its harmonics were reported in IMF, including Earth vicinity (Cane et al., 1998) and most heliophysics data types like solar flares, photospheric magnetic flux, group sunspot numbers, and proton speed, as well as in different ranges depending upon the data, location, epoch, and methodology, as 155–160 days, 160–165 days, 175–188 days, and 180–190 days (Gurgenashvili et al., 2017). Thus, while RR occurs in various ranges, those share the 30–180-day common band. Historically, the Rieger period decreased until the middle of the last century and then began to increase again towards the end of the century, opposite to the activity magnitude trend (Zaqarashvili et al., 2010). Likewise, the Rieger-type periodicities correlate with solar cycle strength and are shorter during solar cycles with higher magnetic activity (Gurgenashvili et al., 2016). This situation implies that RR originates in the Sun engine, as confirmed by Omerbashich (2024).

Since ~2001, Jupiter's decade-scale global magnetoactivity evolution in the RR band took an increasingly sinusoidal form, previously seen in astrophysics as preceding superhumps or superoutbursts (long outbursts) eruptions in dwarf novae (Kuznetsova et al., 1999), and in the pre-bursting magnetar 4U 0142+61 (Omerbashich, 2024). In geology, this rare mode of energy dissipation was noticed in metasomatic metamorphism (Aulbach et al., 2018).

Verifying the directionality of the Jupiter pulsation signal required looking into the Sun's magnetoactivity in the same spectral band (or Rieger resonance) and over the same time interval. Because it lacks large-scale geometries and instead consists mainly of the background field and complex ~10–10^4-km large and up to ~$0.1{\cdot}R_\odot$ high structures, the solar magnetosphere is commonly pluralized as 'magnetic fields'—making computation of any response of the Sun in the band of interest piece-wise (field-by-field) so involved that the MMF was studied instead. While averaging a field does smooth out many intricacies, some still endure in the MMF even though the background field is dominant (Bose & Nagaraju, 2018). Here, that problem was addressed and resolved by GVSA—a robust, rigorous, and gaps-insensitive spectral analysis method.

Sun-like stars with planetary systems expectedly erupt with superflares (Schaefer et al., 2000). While Jupiter-like gaseous giants in close orbits about Sun-like stars could theoretically cause such events, Jupiter appears too remote from the Sun to cause a solar superflare via magnetic tangling under reconnecting (Rubenstein & Schaefer, 2000). However, since the physics of such magnetic reconnections largely remains unknown (*ibid*.), a Jupiter-like gaseous giant with its flaring mechanism (capable of flaring or not), especially if that mechanism were purely magnetic and rotational like Jupiter's, could also entangle its primary star's magnetic field on decadal scales without causing star rotational variations or extinction-level superflares. This particular scenario seems plausible because the geological record does not contain a link between mass extinctions and solar superflares (*ibid*.).

While it is difficult to locate its origin in time, it is easy to see through extrapolation—especially since the solar and thus IMF strengths tended to increase freely after the last (Maunder) grand minimum (Lockwood et al., 1999)—that the Sun–Jupiter decade-scale magnetic entanglement could have had commenced already during one of the previous grand minima. Such extrapolation paints a picture of one star that is otherwise resonant-chaotic (Omerbashich, 2023a) but which, if unchecked, could become far more dangerous than is presently the case. Fortunately, the Sun does appear to be kept in check by a failed star-turned-sub-brown-dwarf Jupiter. In that framework, solar grand minima act as the shutter response of the Sun to a recurring active phase of otherwise inactive pulsar Jupiter. This permanent dance of giants makes Jupiter routinely an indirect but significant Earth climate driver, as supported by observations of stars (de Wit et al., 2017) and the Jupiter orbital geometry, e.g., Niroma (2009).

Besides, if so, there can be little doubt that the Sun had activated this protective mechanism long before humans began observing solar sunspot (local magnetic) activity—possibly while Jupiter was still migrating to its current position inward (for a review of planetary migration models, see, e.g., Raymond

& Morbidelli, 2022). As a here deduced defense mechanism of Sun-like stars, and therefore many normal stars too, the decade-scale magnetic entanglement could explain observations from the Kepler mission according to which only ~1% of gaseous giants orbiting Sun-like stars are hot, whereas ~99% are warm/cold Jupiters.

Given the global and decadal nature of the superflaring mechanism and its recurrence rate along century or longer scales, one can speculate that this star shield from "incoming fire" explains why only <1% of all Jupiters are hot. Namely, besides lowering solar activity, the mechanism possibly also keeps Jupiter at a safe distance by hindering its ability to attain a corrected orbit. This blocking could occur via atmospheric depletion (Lalitha et al., 2018) or Jupiter scattering more mass during grand minima (due to lower production of the solar wind) than it accrues (Adams, 2011), or by preventing Jupiter from clenching onto the Sun magnetism, or in a combination of the above. When unrestrained, either of these primary ways (gravitational and electromagnetic) could enable Jupiter to climb its distance to the Sun. If so, then this last solar line of defense against migrating Jupiters is more likely than not a universal stellar mechanism for preventing gaseous giants from ever leeching on, i.e., becoming hot Jupiters via penetrating the star defenses and assuming a <0.1 AU orbit when the very existence of that star and its planetary system could become jeopardized. In turn, our forever banished Jupiter (and, by extension, Jupiters around normal stars of moderate mass in most cases as deprived of proximity to their unlikely binary companions) lack(s) as such any potential for firing extinction-level superflares. On the other hand, both solar and Jovian uneven bursts still could be expected, but as constrained by a mutual balance.

5. Conclusions

Even though the heliosphere hosts several gaseous giants, the Sun lacks extinction-level superflaring ability observed throughout the known universe. This level of hospitality from the human perspective (and a here newly indicated fundamental criterion for life to exist elsewhere) is likely due to the Sun's protective shutter mechanism akin to a car shock absorber but with the appearance of a camera lens cover and which signals the Sun to lower its magnetic activity when in danger from an incoming star. Specifically, as soon as it recognizes the astrophysical (star-) signature of a decadal energy influx like Jupiter's magnetar/novae-type evolution impulse, the Sun enters into a sleep mode commonly named grand minimum. This mechanism is primordial and so it gets activated regardless of the approaching enemy's own superbursting potential. To maintain system stability, each dramatic reduction in the Sun's (magnetic) activity and subsequent storing of energy eventually ends in the Sun's venting out a superburst of energy from its suppressed global activity—a superflare. This tangling mechanism is also a locking one, as it effectively prevents the Sun from firing extinction-level solar superflares that would normally erupt if Jupiter traveled on a gravely close but fortunately forbidden orbit.

The Jupiter orbital distance and the absence of superflare-caused extinctions from 0–2-kyr-BP geological record make cataclysmic solar and Jovian superflares less likely. However, the current total locking of the two most powerful astrophysical magnetic fields in the solar system represents an attempt by failed star Jupiter to rephase into its primordial stellar state. It is then plausible that the ongoing episode of Sun–Jupiter magnetic entanglement could indicate an onset of a ~10^{32}-erg (non-extinction) superflare, which appears overdue based on various data.

Finally, astrophysical models of star superflaring need to account for the ability of (pulsing) planets at distances even beyond 0.1 AU to trigger non-extinction superflares. Also, since primordial, the shutting-venting mechanism detected by Omerbashich (2024) and the present study likely represents a universal recurring interstellar mechanism. The discovery explains the Milky Way-observed (and by extension probably universal) ~1:3 relative scarcity of binaries (Lada, 2006) and why binaries, and then multinaries progressively so, occur more often with the stellar mass increase (Gratton et al., 2023), i.e., as this mechanism (which does a remarkably efficient sifting job in dwarfs as the predominant yet less massive star type), weakens naturally in more massive stars or in any place where gravity reigns supreme. The mechanism thus safeguards (via an apparent magnetism buffer effect) most stars against incoming active and inactive stars alike by significantly impeding the uninvited guest's orbit corrections. As such, the newly found mechanism could be essential to our understanding of the origin of Jupiter, star formation processes, and the nature of gravity.

Acknowledgments

I thank two anonymous reviewers for their useful comments. The scientific software LSSA, based on the rigorous spectral analysis method by Vaníček (1969, 1971), was used to compute spectra. LSSA v.5 is available as an open-source version from https:/www2.unb.ca/gge/Research/GRL/LSSA/sourceCode.html.

Data statement

The Wilcox Solar Observatory data can be obtained from: http://wso.stanford.edu/#MeanField. NASA's Space Physics Data Facility and Dr. Adam Szabo (Goddard Space Flight Center) are the providers of the WIND mission data found at: https://omniweb.gsfc.nasa.gov/ftpbrowser/mag_iwa.html and https://cdaweb.gsfc.nasa.gov/pub/data/wind/mfi/ascii/. All data analyzed in this study are in a Supplement in the IEEE *DataPort* repository at https://dx.doi.org/10.21227/cv28-8929.

References

Adams, F.C. (2011) Magnetically controlled outflows from hot Jupiters. *Astrophys. J.* 730:27. https://doi.org/10.1088/0004-637X/730/1/27

Alfvén, H. (1942) Existence of electromagnetic-hydrodynamic waves. *Nature* 150(3805):405–406. https://doi.org/10.1038%2F150405d0

Aulbach, S., Heaman, L.M., Stachel, T. (2018) The Diamondiferous Mantle Root Beneath the Central Slave Craton. Geoscience and Exploration of the Argyle, Bunder, Diavik, and Murowa Diamond Deposits. ISBN 9781629496399. https://doi.org/10.5382/SP.20.15

Bai, T. (2003) Hot Spots for Solar Flares Persisting for Decades: Longitude Distributions of Flares of Cycles 19-23. *Astrophys. J.* 585:1114–1123. https://dx.doi.org/10.1086/346152

Bai T., Cliver E.W. (1990) A 154 day periodicity in the occurrence rate of proton flares. *Astrophys. J.* 363:299–309. https://doi.org/10.1086/169342

Basu, S. (2013) The peculiar solar cycle 24—where do we stand? *J. Phys.* 440:012001. https://doi.org/10.1088/1742-6596/440/1/012001

Bose, S., Nagaraju, K. (2018) On the variability of the Solar Mean Magnetic Field: contributions from various magnetic features on the surface of the Sun. *Astrophys. J.* 862:35. https://doi.org/10.3847/1538-4357/aaccf1

Cane, H.V., Richardson, I.G., von Rosenvinge, T.T. (1998) Interplanetary magnetic field periodicity of ~153 days. *Geophys. Res. Lett.* 25(24):4437–4440. https://doi.org/10.1029/1998GL900208

Carbonell, M., Oliver, R., Ballester, J.L. (1992) Power spectra of gapped time series: a comparison of several methods. *Astron. & Astrophys.* 264:350–360. https://ui.adsabs.harvard.edu/#abs/1992A&A...264..350C

Danilović, S., Vince, I., Vitas, N., Jovanović, P. (2005) Time series analysis of long term full disk observations of the Mn I 539.4 nm solar line. *Serb. Astron. J.* 170:79–88. https://doi.org/10.2298/SAJ0570079D

Gonzalez, M.E., Dib, R., Kaspi, V.M., Woods, P.M., Tam, C.R., et al. (2010) Long-term X-ray changes in the emission from the anomalous X-ray pulsar 4U 0142+61. *Astrophys. J.* 716:1345–1355. https://dx.doi.org/10.1088/0004-637X/716/2/1345

Gratton, R., Squicciarini, V., Nascimbeni, V., Janson, M., Reffert, S., et al. (2023) Multiples among B stars in the Scorpius-Centaurus association. *Astron. Astrophys.* 678:A93. https://doi.org/10.1051/0004-6361/202346806

Griesmeier, J.-M., Stadelmann, A., Penz, T., Lammer, H., Selsis, F., et al. (2004) The effect of tidal locking on the magnetospheric and atmospheric evolution of "Hot Jupiters". *Astron. Astrophys.* 425(2):753–762. https://doi.org/10.1051/0004-6361:2003568

Gurgenashvili, E., Zaqarashvili, T.V., Kukhianidze, V., Oliver, R., Ballester, J.L., et al. (2017) North–South Asymmetry in Rieger-type Periodicity during Solar Cycles 19–23. *Astrophys. J.* 845(2):137–148. https://dx.doi.org/10.3847/1538-4357/aa830a

Gurgenashvili, E., Zaqarashvili, T.V., Kukhianidze, V., Oliver, R., Ballester, J.L., et al. (2016) Rieger-type periodicity during solar cycles 14–24: estimation of dynamo magnetic field strength in the solar interior. *Astrophys. J.* 826(1):55. https://doi.org/10.3847/0004-637X/826/1/55

Kuznetsova, Yu.G., Pavlenko, E.P., Sharipova, L.M., Shugarov, S.Yu. (1999) Observations of Typical, Rare and Unique Phenomena in Close Binaries with Extremal Mass Ratio. *Odessa Astron. Pub.* 12:197–200. https://ui.adsabs.harvard.edu/#abs/1999OAP....12..197K

Lada, C.J. (2006) Stellar Multiplicity and the Initial Mass Function: Most Stars Are Single. *Astrophys. J.* 640(1):L63. https://doi.org/10.1086/503158

Lalitha S., Schmitt, J.H., Dash S. (2018) Atmospheric mass-loss of extrasolar planets orbiting magnetically active host stars. *Mon. Not. R. Astron. Soc.* 477(1):808–815. https://doi.org/10.1093/mnras/sty732

Lepping, R.P., Acũna, M.H., Burlaga, L.F., Farrell, W.M., Slavin, J.A., et al. (1995) The WIND magnetic field investigation. *Space Sci. Rev.* 71:207–229. https://doi.org/10.1007/BF00751330

Lockwood, M., Stamper, R. Wild, M. (1999) A doubling of the Sun's coronal magnetic field during the past 100 years. *Nature* 399:437–439. https://doi.org/10.1038/20867

Maehara, H., Shibayama, T., Notsu, Y., Notsu, S., Honda, S., et al. (2015) Statistical properties of superflares on solar-type stars based on 1-min cadence data. *Earth Planets Space* 67:59. https://doi.org/10.1186/s40623-015-0217-z

Maehara, H., Shibayama, T., Notsu, S., Notsu, Y., Nagao, T., et al. (2012) Superflares on solar-type stars. *Nature* 485:478–481. https://doi.org/10.1038/nature11063

von Neumann, J. (1942) A Further Remark Concerning the Distribution of the Ratio of the Mean Square Successive Difference to the Variance. *Ann. Math. Statist.* 13(1):86–88. https://doi.org/10.1214/aoms/1177731645

von Neumann, J. (1941) Distribution of the Ratio of the Mean Square Successive Difference to the Variance. *Ann. Math. Statist.* 12(4):367–395. https://doi.org/10.1214/aoms/1177731677

Niroma, T. (2009) Understanding Solar Behaviour and its Influence on Climate. In: *Natural drivers of weather and climate*. Special Issue of Energy & Environment 20(1/2):145–159. https://doi.org/10.1260%2F095830509787689114

Omerbashich, M. (2024) Jupiter's primordial beat of superoutbursting stars. *J. Geophys.* 66(1):1–14. https://n2t.net/ark:/88439/x001607

Omerbashich, M. (2023a) The Sun as a revolving-field magnetic alternator with a wobbling-core rotator from real data. *J. Geophys.* 65(1):48–77. https://n2t.net/ark:/88439/x080008

Omerbashich, M. (2023b) Global coupling mechanism of Sun resonant forcing of Mars, Moon, and Earth seismicity. *J. Geophys.* 65(1):1–46. https://n2t.net/ark:/88439/x040901

Omerbashich, M. (2021) Non-marine tetrapod extinctions solve extinction periodicity mystery. *Hist. Biol.* 34(1):188–191. https://doi.org/10.1080/08912963.2021.1907367

Omerbashich, M. (2009) *Method for Measuring Field Dynamics*. US Patent #20090192741, United States Patent and Trademark Office. https://worldwide.espacenet.com/publicationDetails/biblio?CC=US&NR=20090192741A1

Omerbashich, M. (2007) Magnification of mantle resonance as a cause of tectonics. *Geodinamica Acta* 20:6:369–383. https://doi.org/10.3166/ga.20.369-383

Omerbashich, M. (2006) Gauss–Vaníček Spectral Analysis of the Sepkoski Compendium: No New Life Cycles. *Comp. Sci. Eng.* 8(4):26–30. https://doi.org/10.1109/MCSE.2006.68
(Erratum due to journal error. *Comp. Sci. Eng.* 9(4):5–6. https://doi.org/10.1109/MCSE.2007.79;
full text: https://arxiv.org/abs/math-ph/0608014)

Omerbashich, M. (2003) *Earth-model Discrimination Method*. Ph.D. Dissertation, pp.129. ProQuest, USA. https://doi.org/10.6084/m9.figshare.12847304

Pagiatakis, S. (1999) Stochastic significance of peaks in the least-squares spectrum. *J. Geod.* 73:67–78. https://doi.org/10.1007/s001900050220

Pettersen, B.R. (1989) A review of stellar flares and their characteristics. *Sol. Phys.* 121:299–312. https://doi.org/10.1007/BF00161702

Poppenhaeger, K. (2015) *Stellar magnetic activity – Star-Planet Interactions*. Invited review for the CoRoT Symposium 3/Kepler KASC-7 joint meeting. Toulouse, France, July 2014. https://doi.org/10.1051/epjconf/201510105002

Poppenhaeger, K., Schmitt, J.H.M.M. (2011) A correlation between host star activity and planet mass for close-in extrasolar planets? *Astrophys. J.* 735:59. https://doi.org/10.1088/0004-637X/735/1/59

Poppenhaeger, K., Robrade, J., Schmitt, J.H.M.M. (2010) Coronal properties of planet-bearing stars. *Astron. Astrophys.* 515:A98. https://doi.org/10.1051/0004-6361/201014245

Press, W.H., Teukolsky, S.A., Vetterling, W.T., Flannery, B.P. (2007) *Numerical Recipes: The Art of Scientific Computing* (3rd Ed.). Cambridge University Press, United Kingdom. ISBN 9780521880688

Raymond, S.N., Morbidelli, M. (2022) Planet formation: key mechanisms and global models. *arXiv*. https://arxiv.org/abs/2002.05756. In: Biazzo, K., Bozza, V., Mancini, L., Sozzetti, A. (Eds.) *Demographics of Exoplanetary Systems*. Lecture Notes of the 3rd Advanced School on Exoplanetary Science. https://www.springer.com/gp/book/9783030881238

Rieger, E., Share, G.H., Forrest, D.J., Kanbach, G., Reppin, C., et al. (1984) A 154-day periodicity in the occurrence of hard solar flares? *Nature* 312:623–625. https://doi.org/10.1038/312623a0

Rubenstein, E.P., Schaefer, B.E. (2000) Are Superflares on Solar Analogues Caused by Extrasolar Planets? *Astrophys. J.* 529(2):1031. https://doi.org/10.1086/308326

Schaefer, B.E., King, J.R., Deliyannis, C.P. (2000) Superflares on Ordinary Solar-Type Stars. *Astrophys. J.* 529(2):1026. https://doi.org/10.1086/308325

Scharf, C.A. (2010) Possible constraints on exoplanet magnetic field strengths from planet-star interaction. *Astrophys. J.* 722:1547–1555. http://dx.doi.org/10.1088/0004-637X/722/2/1547

Scherrer, P.H., Wilcox, J.M., Svalgaard, L., Duvall, Jr. T.L., Dittmer, P.H., et al. (1977) The mean magnetic field of the Sun: Observations at Stanford. *Sol. Phys.* 54:353–361. https://doi.org/10.1007/BF00159925

Spruit, H.C. (2017) *Essential magnetohydrodynamics for astrophysics. An introduction to magnetohydrodynamics in astrophysics*. Max Planck Institute for Astrophysics report. *arXiv*. https://doi.org/10.48550/arXiv.1301.5572

Taylor, J., Hamilton, S. (1972) Some tests of the Vaníček Method of spectral analysis. *Astrophys. Space Sci.* 17:357–367. https://doi.org/10.1007/BF00642907

Tsurutani, B.T., Gonzalez, W.D., Lakhina, G.S., Alex, S. (2003) The extreme magnetic storm of 1–2 September 1859. *J. Geophys. Res.* 108:1268. https://doi.org/10.1029/2002JA009504

Tu, Z.-L., Yang, M., Zhang, Z.J., Wang, F.Y. (2020) Superflares on Solar-type Stars from the First Year Observation of TESS. *Astrophys. J.* 890:46. https://doi.org/10.3847/1538-4357/ab6606

Usoskin, I.G., Gallet, Y., Lopes, F., Kovaltsov, G.A., Hulot, G. (2016) Solar activity during the Holocene: the Hallstatt cycle and its consequence for grand minima and maxima. *Astron. Astrophys.* 587:A150. http://dx.doi.org/10.1051/0004-6361/201527295

Usoskin, I.G., Solanki, S.K., Kovaltsov, G.A. (2007) Grand minima and maxima of solar activity: new observational constraints. *Astron. Astrophys.* 471(1):301–309. https://doi.org/10.1051/0004-6361:20077704

Vaníček, P. (1969) Approximate Spectral Analysis by Least-Squares Fit. *Astrophys. Space Sci.* 4(4):387–391. https://doi.org/10.1007/BF00651344

Vaníček, P. (1971) Further Development and Properties of the Spectral Analysis by Least-Squares Fit. *Astrophys. Space Sci.* 12(1):10–33. https://doi.org/10.1007/BF00656134

Wells, D.E., Vaníček, P., Pagiatakis, S. (1985) *Least squares spectral analysis revisited*. Department of Geodesy & Geomatics Engineering Technical Report 84, University of New Brunswick, Canada. http://www2.unb.ca/gge/Pubs/TR84.pdf

de Wit, J., Lewis, N.K., Knutson, H.A., Fuller, J., Antoci, V., et al. (2017) Planet-induced Stellar Pulsations in HAT-P-2's Eccentric System. *Astrophys. J. Lett.* 836(2):L17. https://doi.org/10.3847/2041-8213/836/2/L17

Zaqarashvili, T.V., Carbonell, M., Oliver, R., Ballester, J.L. (2010) Magnetic Rossby waves in the solar tachocline and Rieger-type periodicities. *Astrophys. J.* 709(2):749–758. https://doi.org/10.1088/0004-637X/709/2/749.